Bioorganic & Medicinal Chemistry 17 (2009) 6914–6925

Contents lists available at ScienceDirect

Bioorganic & Medicinal Chemistry

journal homepage: www.elsevier.com/locate/bmc

Thienylhalomethylketones: Irreversible glycogen synthase kinase 3 inhibitors as useful pharmacological tools

Daniel I. Perez [a], Santiago Conde [a], Concepción Pérez [a], Carmen Gil [a], Diana Simon [b,c], Francisco Wandosell [b,c], Francisco J. Moreno [c], José L. Gelpí [d], Francisco J. Luque [e], Ana Martínez [a,*]

[a] Instituto de Química Médica-CSIC, Juan de la Cierva 3, 28006 Madrid, Spain
[b] Centro de Investigación Biomédica en Red sobre Enfermedades Neurodegenerativas (CIBERNED), Spain
[c] Centro de Biología Molecular 'Severo Ochoa', CSIC-UAM, Universidad Autonoma de Madrid, 28049 Madrid, Spain
[d] Departamento de Bioquímica y Biología Molecular, Facultad de Biología, Universidad de Barcelona, Avda. Diagonal 645, 08028 Barcelona, Spain
[e] Departamento de Fisicoquímica e Instituto de Biomedicina (IBUB), Facultad de Farmacia, Universidad de Barcelona, Avda. Diagonal 643, 08028 Barcelona, Spain

ARTICLE INFO

Article history:
Received 1 April 2009
Revised 21 July 2009
Accepted 13 August 2009
Available online 22 August 2009

Keywords:
GSK-3β inhibitors
Alzheimer's disease
Halomethylketones
Tau phosphorylation

ABSTRACT

Thienylhalomethylketones, whose chemical, biological, and pharmaceutical data are here reported, are the first irreversible inhibitors of GSK-3β described to date. Their inhibitory activity is likely related to the cysteine residue present in the ATP-binding site, which is proposed as a relevant residue for modulation of GSK-3 activity. The good cell permeability of the compounds allows them to be used in different cell models. Overall, the results presented here support the potential use of halomethylketones as pharmacological tools for the study of GSK-3β functions and suggest a new mechanism for GSK-3β inhibition that may be considered for further drug design.

1. Introduction

Human cells contain 491 different protein kinases, which are responsible for phosphorylating certain amino acids. These enzymes are critically involved in a wide variety of cellular processes, including metabolism, transcription, and cell movement. They are linked to a number of diseases, making them important drug targets.[1] Nearly all kinase inhibitors developed so far target the binding site for the nucleotide adenosine 5′-triphosphate (ATP),[2] which has a similar structure in all protein kinases and makes kinase inhibitors unspecific. However, the search for inhibitors of protein kinases has recently culminated in the registration of several compounds such as imatinib (gleevec),[3] or erlotinib (tarceva),[4] for certain cancer therapies. The challenge now is to develop kinase inhibitors for other therapeutic indications where an urgent need for effective treatment is required.[5] Neurodegenerative diseases are one of such indications.

Alzheimer's disease (AD) is the most common cause of dementia in adults. The current therapy for AD has only moderate efficacy in the palliative treatment of the disease, but an effective therapeutic approach is not available yet.[6] Recent studies have suggested the central role of glycogen synthase kinase 3β (GSK-3β) in the pathogenesis of both sporadic and familial forms of AD.[7] GSK-3β is a serine/threonine kinase involved in many cellular signaling pathways. Although it has been known for more than 30 years ago for its participation in glycogen synthesis, it has recently emerged as one of the most fascinating targets for medicinal chemists.[8,9] Today it is well recognized that GSK-3β over-activity is related to several unmet diseases such as type II diabetes, chronic inflammatory diseases and AD. Consequently, its specific inhibitors could be powerful drugs for the effective treatments of such severe pathologies.[10,11]

In AD, the over-activity and/or over-expression of GSK-3β accounts for memory impairment, tau hyperphosphorylation, increased β-amyloid production and local plaque-associated microglial-mediated inflammatory responses which are characteristic hallmarks of the disease.[7] As a causal mediator of AD, inhibitors of GSK-3β would provide a novel avenue for therapeutic intervention in this devastating disorder.[12] Currently, only one compound with this mechanism of action is in clinical trials for AD. The thiadiazolidindione (TDZD) candidate called NP-12 has completed phase I clinical trials with single and multiple doses studies and phase II studies for AD has now started in Europe. A pivotal study on progressive supranuclear palsy, where abnormal hyperphosphorylation of tau in the brain plays a vital role in its molecular pathogenesis,[13] is also planned.

Our research group has been involved for many years in disease-modifying therapeutic approaches for the treatment of AD.[14,15] One of our most active programs is focused on the search,

* Corresponding author. Tel.: +34 91 5854624; fax: +34 91 5644853.
E-mail address: amartinez@iqm.csic.es (A. Martínez).

0968-0896/$ - see front matter © 2009 Elsevier Ltd. All rights reserved.
doi:10.1016/j.bmc.2009.08.042

design, synthesis, and evaluation of GSK-3 inhibitors, which led to the first ATP non-competitive GSK-3β inhibitors known to date.[16] In this manuscript chemical, biological, and pharmaceutical data about thienylhalomethylketones are reported. The results support the use of these compounds as useful pharmacological tools with good cell permeability to gain insight into the role played by GSK-3β in physiological and pathological processes.

2. Results and discussion

2.1. Lead discovery

Our first hit in this series of compounds was discovered searching for GSK-3 inhibitors in our compound library. Preliminary results together with structure–activity relationships studies of this new family of compounds were published in a previous work.[17] Herein we report the synthesis of new compounds (**37**–**44**) and additional experiments carried out for the HMK family.

In the previous work, the initial search was focused on eight unrelated chemical structures (compounds **1–8,** Fig. 1). Commercially available GSK-3β was incubated with ATP and the small peptide GS-1 (based on residues of glycogen synthase phosphorylated by GSK-3β)[18] as substrate, in the presence and absence of the compound, and the inhibitory activity was measured following a previously described method.[18] GSK-3β activity was expressed as picomoles of phosphate incorporated per 20 min of incubation or as the percentage of maximal activity. All the compounds tested were inactive or poorly active other than 2-chloroacetyl-4,5-dichlorothiophene **8**, which inhibited GSK-3β at a very low concentration.

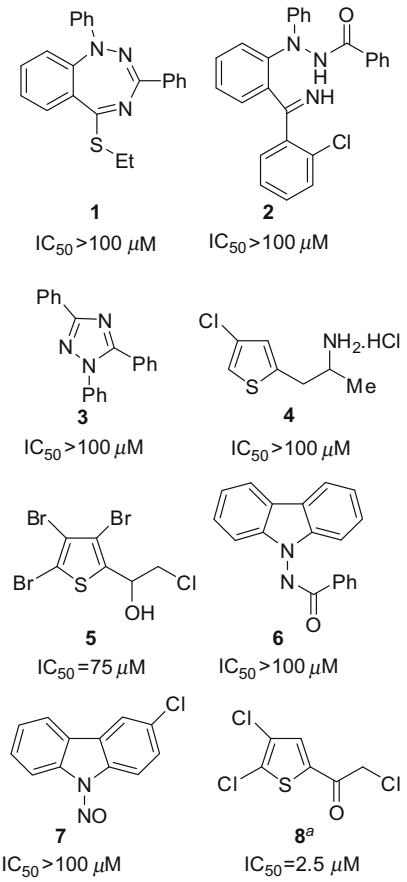

Figure 1. First compounds used for the GSK-3β inhibition screening with their experimental IC_{50} values. [a]Ref. 17.

Based on this encouraging finding, a second set of 13 compounds was selected from our library and those bearing a thiophene or phenyl ring with a carbonyl moiety directly attached were further tested. The highest activities were found for the group of chloromethylhalothienyl ketones (chloroacetylhalothiophenes **19–21**; Fig. 2), while non-halogenated alkyl ketones, esters, and aldehydes did not inhibit GSK-3β at the maximum concentration used (100 μM). These data suggested that the chloroacetylthiophene moiety could be a structural feature required for activity, and it was selected as a chemical scaffold for lead optimization.

2.2. Lead optimization and SAR

To explore the structure–activity relationships (SAR) on this new class of GSK-3β inhibitors, a variety of 2- or 3-substituted halomethylthienylketones (Scheme 1) were synthesized.

We first examined the effect of some substituents, mainly alkyl or halide, on the thiophene heterocycle. These compounds, although previously known, were here synthesized by chloroacetylation of the corresponding thiophene following the Friedel–Crafts method (compounds **22–36**; Scheme 1) to be evaluated as GSK-3 inhibitors. In some cases, when 2.1 equivalents of chloroacetyl chloride and aluminum trichloride were used, mixtures of mono- and di-chloroacylated compounds were obtained (compounds **22**–**28**). Isolation was then performed by chromatographic techniques and the chemical structure unequivocally elucidated by their spectroscopic properties. GSK-3β inhibitory activities of all the 15-substituted chloromethyl thienyl ketones prepared are presented in Table 1.

Besides the chloroacetyl group, a second substituent is required to enhance activity, as noted in the comparison of the activities measured for compound **22** versus the activity of **21** and **8**. Moreover, this second substituent must be electron-withdrawing, such as halide atoms or chloroacetyl groups, in order to maintain or increase the inhibition of GSK-3β. Thus, when an electron-donating group such as the methyl moiety is present (compounds **24**, **26**, **27**, **36**), the inhibition of GSK-3β is very low or completely lost. This fact might suggest that the electron distribution on the molecular surface should be important for the inhibitory activity, as also noted for TDZDs derivatives.[19]

To further examine the influence of the chloroacetyl moiety on GSK-3β inhibition, derivatives **37, 38**, and **43**, in which the distance between the carbonyl group and the halide atom is enlarged, were synthesized. For the synthesis of these compounds 4-chlorobutyryl chloride was used as acylating agent. In vitro evaluation showed a complete lack of activity (Table 2).

Furthermore, the nature of the halide atom joined to the acetyl moiety was also explored. Different substituted bromomethyl thienyl ketones **39–42** were synthesized employing bromoacetyl bromide, all of them being inhibitors of GSK-3β. While the change of chlorine by bromine does not alter the IC_{50} (compounds **39–42**), substitution by an ester moiety (**44**) led to a drastic decrease in inhibitory activity (Table 2), which points out that the halide atom is crucial for activity. Compound **44** was synthesized when chloroacetylthiophene **35** reacted in the presence of sodium acetate and sodium anhydride in acetic acid (Scheme 1). The substitution of the halide atom in the chloroacetyl chain confirms the halomethylketone (HMK) moiety as the structural feature required for activity.

Considering the HMK chemical feature key for GSK-3β inhibition and the Hammett inductive substituent constant (σ_I), we can explain the lack of activity for methyl-substituted thiophenes ($\sigma_I = -0.17$) and the activity of chloro-, bromo- and chloroacetyl-substituted thiophenes ($\sigma_I = 0.23$, 0.23, and 0.50, respectively) as a consequence of their electronic influence on the reactivity of HMK moiety directly attached to the aromatic ring.

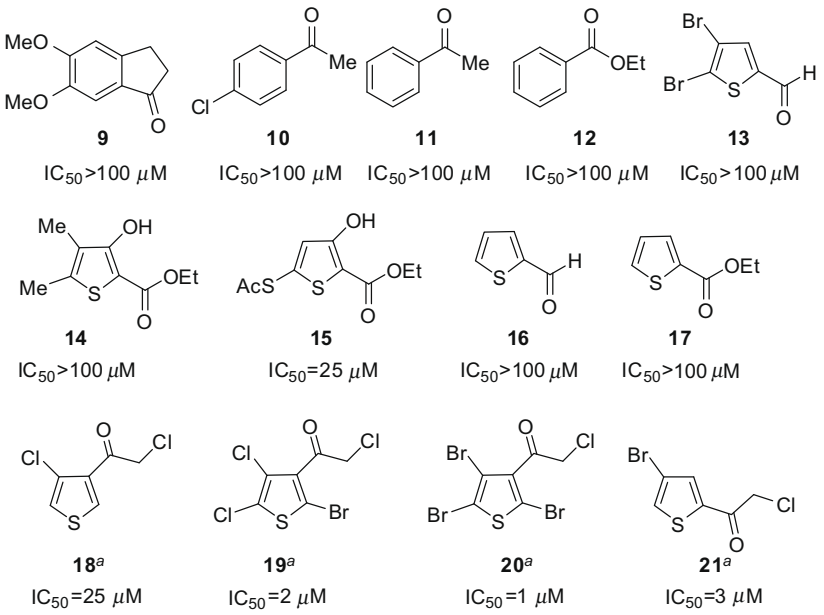

Figure 2. Focused library used in discovery of GSK-3β inhibitors with their experimental IC_{50} values. [a]Ref. 17.

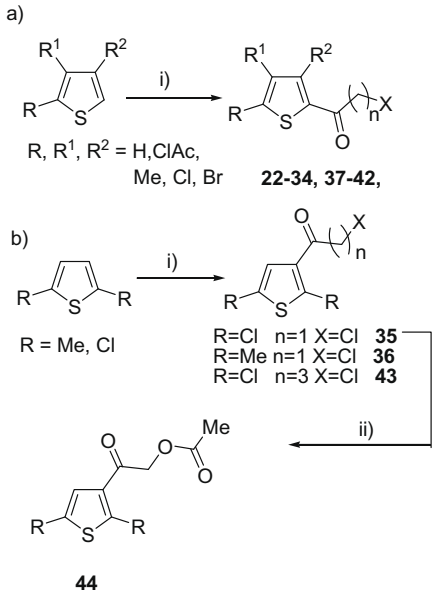

Scheme 1. Synthesis of compounds **22–44**. Reagents and conditions: (i) $XCO(CH_2)_nX$, $AlCl_3$, CS_2, (ii) $(AcO)_2O$, NaOAc, AcOH, Δ.

Table 1
Inhibition of GSK-3 by chloromethyl thienyl ketones[a]

Compd	R	R^1	R^2	IC_{50} (μM)
		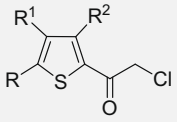		
22	H	H	H	50
23	H	ClAc	H	1.5
24	Me	H	H	>100
25	Me	ClAc	H	5.0
26	H	H	Me	75
27	H	Me	H	>100
28	H	ClAc	Me	5.0
29	Cl	H	H	10
30	Br	H	H	10
31	H	Br	Br	0.5
32	Br	Br	H	1.0
33	Ac	H	H	50
34	H	Ac	H	8.0
		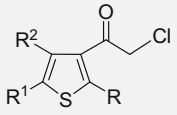		
35	Cl	Cl	H	5.0
36	Me	Me	H	>100

[a] Ref. 17.

2.3. Mechanism of GSK-3 inhibition and selectivity

2.3.1. Kinetic studies on GSK-3β

To investigate the inhibitory mechanism of HMKs on GSK-3β and further confirm our previous results, several kinetic experiments were performed using two different HMKs (compounds **19** and **23**). Lineweaver–Burk plots of enzyme kinetics are shown in Figure 3.

Kinetic experiments varying both ATP levels (6.5, 10, 15 25, 50, and 100 μM) and HMKs (1 and 2 μM) were performed. Double-reciprocal plotting of the data are depicted in Figure 3a. The intercept of the plot in the vertical axis ($1/V$) rises when the HMK concentration increases (from 1 to 3 μM), whereas the intercept in the horizontal axis ($1/S$) does not change, meaning that, while the enzyme maximal rate (V_{max}) decreases in the presence of the inhibitor, the Michaelis–Menten constant (K_m) remains unaltered. These results would suggest that HMKs act as non-competitive inhibitors of ATP binding, because an increase in the ATP concentration (from 6.5 to 100 μM) does not interfere with enzymatic inhibition.

We have also studied the substrate dependence of the kinase activity in the presence of these inhibitors using the peptide GS-1 as substrate. Kinetic experiments were performed varying the concentrations of both GS-1 (6.5, 10, 15, 25, 50, and 100 μM) and inhibitors **19** and **23** (from 1 to 2 μM), while the ATP concentration was kept constant (15 μM). Double-reciprocal plotting of the data

Table 2
Inhibition of GSK-3 by substituted thiophenes

Compd	R	R^1	R^2	*n*	X	IC_{50} (μM)
		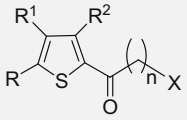				
37	Cl	H	H	3	Cl	>100
38	Br	H	H	3	Cl	>100
39	H	Br	Br	1	Br	1.0
40	Br	Br	H	1	Br	1.0
41	Br	H	H	1	Br	1.0
42	Br	H	Br	1	Br	1.0
		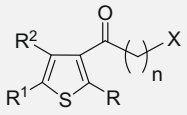				
43	Cl	Cl	H	3	Cl	>100
44	Cl	Cl	H	1	OCOMe	>100

(Fig. 3b), in which each point is the mean of three different experiments, suggest that HMKs act also as non-competitive inhibitors of GS-1 binding.

2.3.2. Kinase profiling

Selectivity of kinase inhibition is critical for pathway analysis in vivo and in cellular systems. To examine the selectivity of these compounds for GSK-3β, many of them (compounds **18, 19, 23, 25, 28–32, 34, 35, 39**, and **40**) were tested as inhibitors of serine/threonine cAMP-dependent protein kinase (PKA). All of them remained inactive at the highest concentration (100 μM) used. Furthermore, the same set of compounds was evaluated against a panel of eight different serine/threonine and tyrosine kinases (CaM-K II, MAP-K, EGFR-K, IR-K MeK1-K, Abl-K, PKp56, and Src). These kinases are involved in very different signaling pathways implicated not only in neurodegeneration (Cam-KII and MAP-K) but also in other physiological processes and diseases as insulin signal pathway (IR-K) or cancer (Abl-K, EGFR-K, MeK1-K, and Src). The inhibitory assays were performed using a 10 μM concentration for the different inhibitors. The results reported in Table 3 show that, in general, HMKs do not exhibit a significant inhibitory effect on the whole set of kinases, except in the proto-oncogenic Src, which is elevated in some human tumors.

2.3.3. Neurotransmitter receptors binding

In order to determine the potential off-target effects of these GSK-3β inhibitors, due to the chemical structure of our leads or to the enzyme targeted, we evaluated the in vitro binding to different neurotransmitter receptors. We selected α-adrenergic (α_2), dopaminergic (*h*D2 and *h*D3), glutamatergic (AMPA and NMDA), muscarinic (*h*M), nicotinic (bungarotoxin sensitive and insensitive), and serotoninergic (5-HT) receptors. Human recombinant

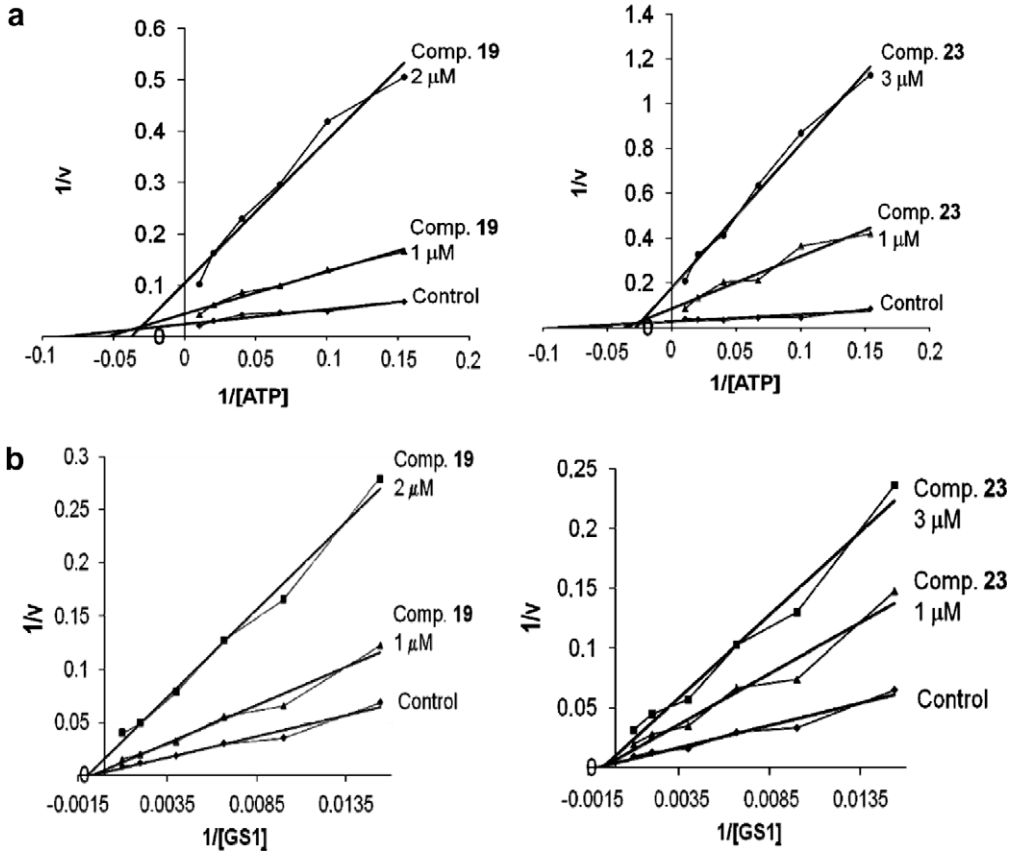

Figure 3. Double-reciprocal plots of kinetic data from assays of GSK-3β activity at different concentrations of HMKs (**19** and **23**). (a) ATP concentrations in the reaction mixture varied from 6.5 to 100 μM. HMKs concentrations are depicted in the plot, and the concentration of GS-1 was kept constant at 15 μM. V is picomoles of phosphate/20 min. (b) GS-1 concentrations in the reaction mixture varied from 6.5 to 100 μM. HMKs concentrations are depicted in the plot, and the concentration of ATP was kept constant at 15 μM. V is picomoles of phosphate/20 min.

Table 3
Inhibitory activity (%inhibition)[a] exhibited by selected HMKs compounds for several kinases

Compd (10 μM)	Abl-K	CAM-K II	EGFR-K	IR-K	MAP-K	MEK 1 K	PK p56	Src-K
18	–	–	–	–	–	–	31	24
19	–	–	–	–	–	–	33	26
23	–	21	16	12	–	–	49	94
25	–	–	25	12	–	–	17	54
28	–	19	–	11	–	16	–	61
29	–	–	–	–	–	–	–	–
30	–	16	–	–	–	–	–	19
31	–	–	–	–	–	–	20	n.d
32	–	–	–	–	–	–	–	69
34	–	–	–	–	–	12	–	22
35	–	10	–	–	–	–	41	12
39	–	–	17	–	–	–	–	66
40	–	–	–	12	–	–	–	76

[a] The symbol – indicates an inhibition of less than 10%. n.d. value not determined because of interference with the detection method due to compound autofluorescence.

ones were selected when available. The results (see Table 4) show that HMKs do not bind to any of these biological targets, thus reducing the potential secondary effects in vivo and pointing to a selective mechanism of action.

2.3.4. Enzyme mapping

To gain deeper insight into the inhibitory mechanism of HMKs to GSK-3β, a mapping study was performed to identify potential cavities suitable for binding. To this end, the docking module of classical molecular interaction potential (CMIP) program[20] was used, taking advantage of the availability of X-ray crystallographic data for GSK-3β. This computational approach has been previously validated for several chemically diverse GSK-3 inhibitors whose binding mode had been previously determined by solving the X-ray structure of the complexes with GSK-3β.[19] The CMIP analysis was performed for the active HMK **32** and the inactive and chemically related derivative **16**. While there seems to be a rather unspecific interaction with HMK **16**, which could reflect its lack of GSK-3β inhibition, a binding site is found for **32** near the ATP-binding site (see Supplementary data). To further check this finding, the interaction of **32** at the ATP-binding site was reexamined by means of alternative docking studies performed with rDock. In one of the two main clusters of poses, **32** is inserted in a highly hydrophobic pocket (formed by residues Ile62, Val70, Ala83, Met101, Val110, Leu132, Tyr134, Val 135, and Leu188) at the rear of the ATP-binding site, and the carbon atom bearing the chlorine is positioned above the sulfur atom of Cys199 (distance of 3.7 Å; see Fig. 4).

This binding mode might not a priori justify the non-ATP competitive nature of HMKs. However, the presence of the thiol group of Cys199, lying close to the HMK in some of the structures docked into the ATP-binding site suggests an alternative interpretation to the mechanism of action of HMKs. Although cysteine residues within active sites of kinases are relatively rare, several cases are well known,[21,22] and the glutathionylation of cysteines present in the activation loop is a general regulation mechanism for protein kinases.[23] Moreover, recent studies revealed that a unique active site cysteine (Cys199) is present in GSK-3β, which is replaced by other residues in other kinases, such as alanine in cycline dependent kinase 2 (CDK-2; see Fig. 5).[24]

Considering this unique structural motif on GSK-3 and the ability of peptidyl-HMKs to inhibit serine[25] and cysteine[26] proteases, we propose a covalent interaction between Cys199 and HMKs in their specific binding to GSK-3. This should consist in the formation of a thioether carbon–sulfur (C–S) bond and subsequent elimination of the halide atom, which might be favored by the stabilization of the leaving chloride anion by the protonated amino group of Lys85 (Fig. 4). The covalent modification here proposed may explain the observed inhibitory kinetics and kinase selectivity. Among the kinases assayed, only Src was inhibited by HMKs. The chemical feature critical for Src activity is a specific cysteine cluster in the catalytic site.[27] Therefore, a covalent modification by HMKs could inhibit this tyrosine kinase.

Modification of this unique cysteine on the GSK-3 catalytic site has been postulated previously, although not demonstrated, in other thiol-reactive compounds.[28] We propose here that Cys199 can be a key residue for modulation of GSK-3β activity and offers

Table 4
Inhibitory activity (%inhibition)[a] exhibited by selected HMKs compounds for several neurotransmitter receptors

Compd (10 μM)	α2	H D2	H D3	AMPA	NMDA	M	N (αBGT insensitive)	N (αBGT sensitive)	5 HT
18	–	13	–	–	16	–	–	–	–
19	–	31	–	–	13	–	–	–	–
23	10	–	–	25	–	–	–	–	–
25	–	–	–	–	–	–	–	–	–
28	–	–	–	–	10	–	11	–	–
29	–	–	–	17	–	–	–	–	–
30	–	–	–	–	–	–	–	–	–
31	–	–	12	–	–	11	–	–	–
32	–	–	–	–	–	–	–	–	–
34	–	–	–	–	–	–	17	–	–
35	–	–	–	17	–	–	–	–	12
39	–	–	–	–	–	–	22	–	–
40	–	–	–	–	–	–	–	–	–

[a] The symbol – indicates an inhibition of less than 10%.

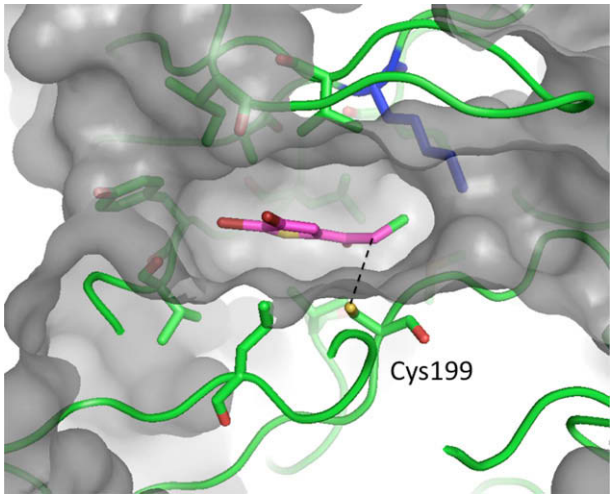

Figure 4. Representation of the putative binding mode of HMK **32** in the ATP-binding site of GSK-3β. The inhibitor fits a hydrophobic cavity (surface in gray) delineated by hydrophobic residues (shown green). The carbon atom bearing the chloride is above the sulfur atom of Cys199, and the chlorine atom is close to the amino group of Lys85 (shown in blue).

a new way to selectively target this important enzyme. According to the previous SAR and the GSK-3 3D surface potential maps,[29] it is reasonable to hypothesize that HMKs inhibitors are first recognized near the enzymatic catalytic site and subsequently modify covalently the specific Cys199. Further studies are in progress, including directed mutagenesis to confirm these first results.

2.3.5. Chemical reactivity of HMKs versus thiol groups

Halomethylketones have been classified as reactive chemical groups. To study to some extent the potential reactivity of these compounds, we analyzed the reaction between the HMK **29** and mercaptoethanol. Reactions were carried out at room temperature and the progress was followed by HPLC–MS. In a HMK **29**/mercaptoethanol (1:1) reaction mixture, no S-alkylated product was found after 30 min. Only 7% of the sulfur derivative was detected when the mixture was stirring for 24 h. When the concentration of mercaptoethanol was increased 10-fold, 16% of the S-alkylated product was formed after 18 h. However, in equimolar concentrations of HMK **29** and mercaptoethanol, when a tertiary amine was present in the reaction media, 75% of the S-alkylated product was observed after the first 30 min. These results confirm that the reactivity of our HMKs versus thiol groups is mediated by a basic environment and explain the crucial role of Lys85 in the binding of our HMKs to Cys199 in the ATP site of GSK-3β.

2.3.6. Derivatization of sulfhydryl groups on GSK-3

To check the relevance of Cys199 in the inhibition of GSK-3 we have alkylated the free thiol groups in GSK-3β by the treatment with iodoacetamide. We have observed a complete lack of activity after this treatment, showing the relevance of this chemical motif in mediating the inhibition mechanism of the enzyme. Two different inhibitors, lithium and the HMK **32** were used as control (Fig. 6).

```
GSK3-beta  110  VRLRYFFYSSGEKKD-EVYLNLVLDYVPETVYRVARHYSRAKQ-TLPVIYVKLYMYQLFR  167
GSK3-alpha 173  VRLRYFFYSSGEKKD-ELYLNLVLEYVPETVYRVARHFTKAKL-TIPILYVKVYMYQLFR  230
CDK-1       64  VSLQDVLMQDSR-------LYLIFEFLSMDLKKYLDSIPPG-Q-YMDSSLVKSYLYQILQ  114
CDK-2       64  VKLLDVIHTENK-------LYLVFEFLHQDLKKFMD--ASALT-GIPLPLIKSYLFQLLQ  113
CDK-5       64  VRLHDVLHS--DKK-----LTLVFEFCDQDL---KKYFDSCNG-DLDPEIVKSFLFQLLK  112

GSK3-beta  168  SLAYIHSFGICHRDIKPQNLLLDPDTAVLKLCDFGSAKQLVRGEPNVSY---ICSRYYRA  224
GSK3-alpha 231  SLAYIHSQGVCHRDIKPQNLLVDPDTAVLKLCDFGSAKQLVRGEPNVSY---ICSRYYRA  287
CDK-1      115  GIVFCHSRRVLHRDLKPQNLLID-DKGTIKLADFGLARAF--GIPIRVYTHEVVTLWYRS  171
CDK-2      114  GLAFCHSHRVLHRDLKPQNLLINTEGAI-KLADFGLARAF--GVPVRTYTHEVVTLWYRA  170
CDK-5      113  GLGFCHSRNVLHRDLKPQNLLINRN-GELKLADFGLARAF--GIPVRCYSAEVVTLWYRP  169

GSK3-beta  225  PELIFGATDYTSSIDVWSAGCVLAELL-LGQPIFPGDSGVDQLVEIIKVLGTPTREQIRE  283
GSK3-alpha 288  PELIFGATDYTSSIDVWSAGCVLAELL-LGQPIFPGDSGVDQLVEIIKVLGTPTREQIRE  346
CDK-1      172  PEVLLGSARYSTPVDIWSIGTIFAELA-TKKPLFHGDSEIDQLFRIFRALGTPNNEVWPE  230
CDK-2      171  PEILLGCKYYSTAVDIWSLGCIFAEMV-TRRALFPGDSEIDQLFRIFRTLGTPD-EVVWP  228
CDK-5      170  PDVLFGAKLYSTSIDMWSAGCIFAELANAGRPLFPGNDVDDQLKRIFRLLGTPTEEQWPS  229
```

Figure 5. The unique Cys residue near the ATP-biding site in GSK-3 (α and β) is shown by their alignment with different CDKs.

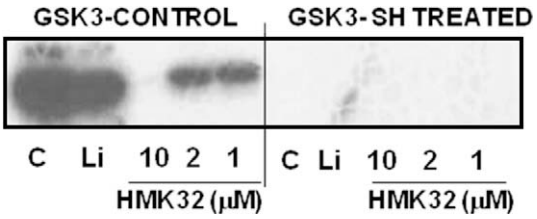

Figure 6. The sulfhydryl groups of GSK-3β were derivatized by reaction with iodoacetamide. The kinase activity from GSK-3 derivatized by iodoacetamide (GSK-3-SH TREATED), or without any modification (GSK-3-CONTROL) was assayed with myelin binding protein. The autoradiography shows that HMK **32** reduced the kinase activity, in the range of 1–10 mM, and that GSK-3 treated with iodoacetamide (GSK-3-SH TREATED) lost its kinase activity.

2.3.7. Reversibility studies

To confirm experimentally the irreversible enzymatic inhibition hypothesized for HMKs, we have studied the recovery of GSK-3β activity after HMK treatment. To this end, an immobilized recombinant histidine-tagged GSK-3β on a nickel agarose gel was used, and the activity of the solid-supported enzyme was measured by the scintillation method. In the presence of HMKs **19** and **32**, a reduction of the phosphorylation activity was observed (after 20 min the activity was only 20% of the maximal phosphorylation activity). Then, several careful washes were performed on the immobilized enzyme to eliminate the inhibitor and the enzymatic activity was subsequently measured. The GSK-3β phosphorylating ability was not recovered, suggesting that the inhibitor remains irreversibly bound to the enzyme.

Moreover, a second experiment was performed using recombinant GSK-3β in solution. In that case, we pre-incubated for 30 min the enzyme and the HMK **32.** Then, the reaction mixture was diluted 20 times and the final kinase activity determined. Control was used following the same strategy but without inhibitor. We have found a complete lack of activity after the HMK pretreatment, showing a potential covalent or very strong binding to the enzyme (Fig. 7).

These findings suggest that HMKs are the first irreversible GSK-3β inhibitors described up to now, leading to a new interpretation of the plots depicted in Figure 3a. When GSK-3β is incubated in the presence of an HMK derivative, covalent modification of Cys199 abolishes its phosphorylating activity, presumably by altering the correct positioning of ATP in the ATP-binding site, thus explaining why an increase in ATP concentration does not vary the enzymatic inhibition.

2.4. Cellular effects of GSK-3 inhibition

To evaluate the cell permeability of HMK inhibitors and their potential use as pharmacological tools and/or leads for drug design, we further explored their effect on tau phosphorylation and neuritogenesis.

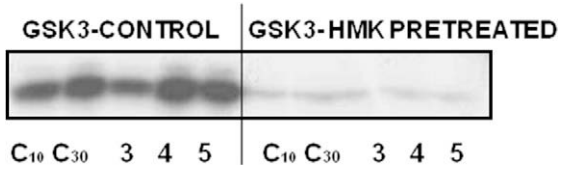

Figure 7. GSK-3β was incubated with HMK **32** (10 μM), afterward was diluted 20 times and then the kinase activity assayed. The kinase activity of GSK-3 pre-inhibited (GSK-3-HMK PRE-TREATED); or without any previous inhibition (GSK-3-CONTROL) were assayed using MBP, as substrate. The autoradiography shows the kinase activity, in both circumstances, after 10 or 30 min of reaction (C10, C30). Subsequent addition of HMK **32** at 10 μM (3), or lithium chloride at 1 mM (4) or HMK **32** (0.5 μM) (5) were also shown.

2.4.1. Tau phosphorylation

Since GSK-3β is shown to phosphorylate tau both in transfected cells and in vivo,[30] the ability of HMKs to interfere with the GSK-3β-mediated tau phosphorylation in cells was explored using primary granule cerebellar neurons (GCNs).

The effect of HMK addition on tau phosphorylation was determined by Western blotting. Detection was carried out using the PHF-1 phosphospecific antibody and Tau-1 (see Section 4). Lithium chloride was added as positive control to the medium at 10 mM. The bands were quantified by densitometric analysis. Data showed that the addition of different HMKs (compounds **18, 19, 23, 28–30**, and **32**) reduced (PHF-1) or increased (Tau-1) the tau-immunoreactivity (see Fig. 8). The effect of HMKs on tau phosphorylation was similar to the trend observed when lithium chloride was used as a GSK-3β inhibitor (IC_{50} 1.5 mM).

2.4.2. Increased neuritogenesis

GSK-3β is involved in cellular differentiation processes and promotes neurite outgrowth in different cell lines.[31] In some neuroblastoma cell lines, such as N2A, a neuronal-like phenotype may be generated by either incubation in a serum-free medium, or by lithium chloride treatment in the presence of serum (DEMEN-10%FCS). To evaluate whether some HMKs may have a similar lithium-like effect, we added these compounds to N2A in the presence of serum. As indicated in Figure 9, treatment of N2A cell cultures with compounds **19** and **23** for 16 h showed an increase in neurite outgrowth. These results suggest that HMKs may have similar intracellular targets as lithium chloride and indirectly show good cell permeability.

2.5. ADME properties

Early ADME considerations in preclinical development would help to avoid costly late stage preclinical and clinical failures, and a number of in silico, in vitro and in vivo techniques are available to screen compounds for ADME characteristics.[32,33] For our purposes, the oral absorption and blood brain barrier permeability properties of HMKs were explored using the previously reported CODES/neural network methodology, which was able to predict those properties for structurally diverse drugs.[34] Using our in silico ADME model based on CODEs descriptors, we have determined that compounds **29** and **35** are able to cross the blood brain barrier and be orally absorbed (see Table 5). Therefore, HMKs have potential value to be used in animal studies aimed at determining the functional implications of GSK-3 in certain neurological disorders. At this point it is worth noting that peptidyl chloromethylketones, which have limited biological utility due to their potential toxicity, are useful tools to study processes mediated by cysteine protease in animal models.[35]

3. Conclusions

HMKs represent a new family of GSK-3β inhibitors that are the first irreversible inhibitors reported to date for this therapeutically valuable kinase. We postulate that their inhibitory activity is mediated by covalent modification of Cys199 residue, which might represent a new strategy to be considered for the future design of new specific GSK-3 inhibitors. We have also shown their ability to promote neurite outgrowth and to decrease tau phosphorylation. In addition, they exhibit the ability to activate the promoter IV of brain-derived growth factor on neurons.[36] Furthermore, these compounds are predicted to cross the blood–brain barrier, increasing their value as tools to be used in animal models for neurodegenerative disorders. Finally, it is worth mentioning that they are now available from several commercial sources, that is, EMD-Cal-

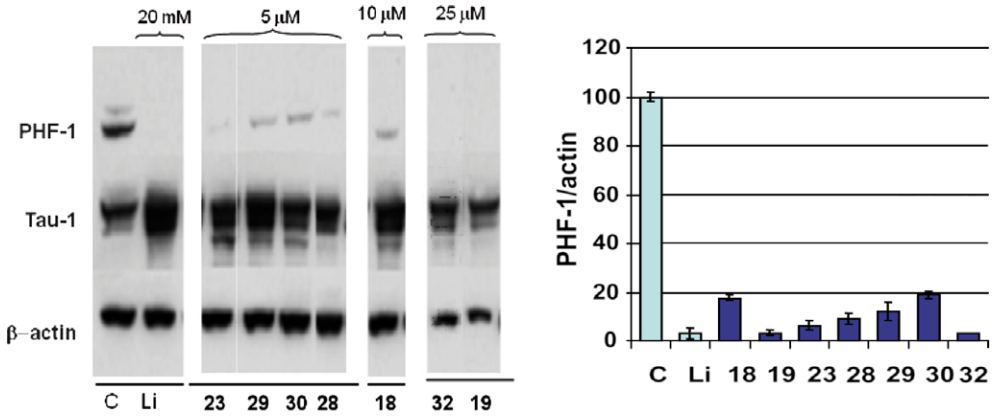

Figure 8. A representative Western blot of soluble extracts from Granule cerebellar neurons (GCNs), obtained after 16 h in the presence of lithium chloride (Li) or different HMKs (compounds **18, 19, 23, 28, 29, 30, 32**). C represents cell extracts from control GCNs. Identical samples were incubated with anti-tau-1, or anti PHF-1; or with anti-β-actin as a loading control. In each experiment, PHF-1 was normalized with respect to the amount of actin present in each cell extract. The data are expressed as the mean of three independent experiments and the data from control cells were considered 100 relative units (r.u.).

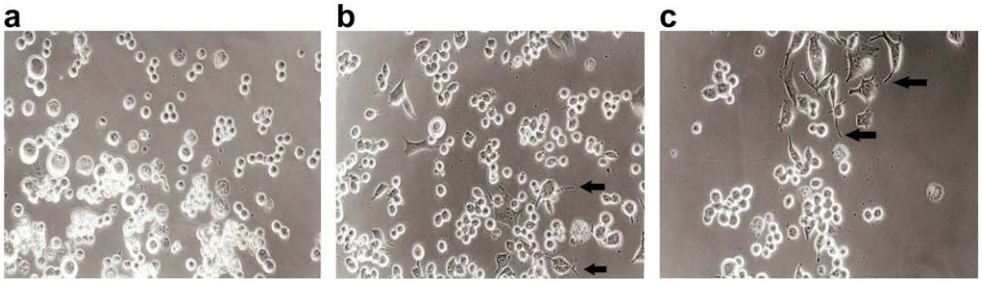

Figure 9. Phase-contrast photography from N2A cells treated for 16 h with different HMKs. (a) Control + DMSO treatment, (b) treatment with compound **23** at 0.2 μM, (c) treatment with compound **19** at 2 μM. The arrows illustrated some cytoplasmic extension detected only after compound **19** or **23** additions (b, c).

Table 5
Predicted percentage of oral absorption and calculated log [BB] for compounds **29** and **35** using neural network/CODES model

Compound	Oral absorption (%)	Log [BB]
29	100	0.166
35	85	0.085

biochem and Merck, as GSK-3β inhibitor VI and VII. These two compounds have been successfully used to study different aspects of GSK-3 functions.[36,37,38] Overall, HMKs represent useful pharmacological tools for use in proof of concept studies for neurological disorders where GSK-3 might be involved.

4. Experimental

4.1. Chemistry

Melting points were determined with a Reichert-Jung Thermovar apparatus and are uncorrected. Flash column chromatography was carried out at medium pressure using silica gel (E. Merck, Grade 60, particle size 0.040–0.063 mm, 230–240 mesh ASTM). Compounds were detected with UV light (254 nm). ^{1}H NMR spectra were obtained on a Gemini-200 spectrometer working at 200 MHz. Typical spectral parameters: spectral width 10 ppm, pulse width 9 μs (57°), data size 32 K. ^{13}C NMR experiments was carried out on the Varian Gemini-200 spectrometer operating at 50 MHz. The acquisition parameters: spectral width 16 kHz, acquisition time 0.99 s, pulse width 9 μs (57°), data size 32 K. Chemical shifts are reported in values (ppm) relative to internal Me_4Si and *J* values are reported in hertz. Elemental analyses were performed by the analytical department at CENQUIOR (CSIC), and the results obtained were within ±0.4% of the theoretical values.

Mass spectra were obtained by electronic impact in a Hewlett–Packard 5973 spectrophotometer.

HPLC analyses for HMKs were performed on a Waters 6000 instrument, with UV detector (214–254 nm), using different columns; Delta Pack C18, 5 μm, 300 Å, (150 × 3.9 mm), μ Bondapack C18, 10 μm, 125 Å, (300 × 3.9 mm) and Symmetry C18, 5 μm, 100 Å, (150 × 3.9 mm). Acetonitrile/H_2O [(0.05% H_3PO_4 + 0.04% Et_3N)] 50/50 was used as mobile phase. For the chemical reactivity of HMKs versus thiol groups, experiments were performed in a Waters 2695 diode array, with positive electrospray using the sunfire column C18, 3.5 μm (50 × 4.6 mm) and acetonitrile (0.08% formic acid) and MiliQ water (0.1% formic acid) as mobile phase in a 10–100 gradient.

The synthesis of chloroacetyl thiophenes 22–36 were previously described[17] and their analytical and spectroscopic data are reported in Supplementary data.

4.1.1. General procedure for the synthesis of 4-chlorobutyrylthiophenes (37, 38, 43) and bromoacetylthiophenes (39–42)

The corresponding thiophene was added to a stirred mixture of 4-chlorobutyryl chloride (compounds **37**, **38**, **43**) or bromoacetyl bromide (BrAcO-Br) (compounds **39**–**42**) and anhydrous aluminum chloride ($AlCl_3$) in dry carbon disulfide (CS_2). Then the mixture was stirred at room temperature overnight, refluxed for 3 h and cooled in an ice bath. Under vigorous stirring, HCl 0.1 N was cautiously

added to this cooled mixture, the present solid disappeared and the reaction mixture separated in two layers. The aqueous layer was extracted with CH_2Cl_2 (50 mL). The organic layers were combined and washed again with water (25 mL), HCl 0.1 N (2 × 15 mL), and a saturated solution of $NaHCO_3$ (15 mL), dried over magnesium sulfate and evaporated. The compounds were purified by column chromatography.

4.1.1.1. 4-Chloro-1-(5-chlorothiophen-2-yl)butan-1-one (37).

4-Chlorobutyryl chloride (3.24 g, 0.023 mol), anhydrous $AlCl_3$ (3.06 g, 0.023 mol), 2-chlorothiophene (2.37 g, 0.020 mol) and dry CS_2 (50 mL). Purified by column chromatography (hexane:ethyl acetate 4:1), 2.06 g (46%), colorless solid, mp 46–47 °C. ^{1}H NMR (200 MHz, $CDCl_3$): δ 7.53 (d, J = 4.0 Hz, 1H, Ar), 6.96 (d, J = 4.0 Hz, 1H, Ar), 3.65 (m, 2H, CH_2), 3.05 (m, 2H, CH_2), 2.20 (m, 2H, CH_2); ^{13}C NMR (50 MHz, $CDCl_3$): δ 191.2 (CO), 142.5 (C–CO), 139.8 (C–Cl), 131.8 (CH), 128.0 (CH), 44.1 (CH_2), 35.0 (CH_2), 26.3 (CH_2); m/z (EI): 226, 224, 222 (M^+, 1, 3, 5%), 147, 145 (M–$CH_2CH_2CH_2Cl$, 38, 100%); HPLC: Column μ Bondapack C18, 10 μm, 125 Å, (300 × 3.9 mm), purity 99%, rt = 4.16 min, acetonitrile/H_2O (0.05% H_3PO_4 + 0.04% Et_3N) 50/50. Anal. Calcd for $C_8H_8Cl_2OS$: C, 43.06; H, 3.61; S, 14.37. Found: C, 42.98; H, 3.49; S, 14.41.

4.1.1.2. 1-(5-Bromothiophen-2-yl)-4-chlorobutan-1-one (38).

4-Chlorobutyryl chloride (3.24 g, 0.023 mol), anhydrous $AlCl_3$ (3.06 g, 0.023 mol), 2-bromothiophene (3.26 g, 0.020 mol) and dry CS_2 (50 mL). Purified by column chromatography (hexane:ethyl acetate 4:1), 2.00 g (38%), colorless solid, mp 43–44 °C. ^{1}H NMR (200 MHz, $CDCl_3$): δ 7.40 (d, J = 4.0 Hz, 1H, Ar), 7.05 (d, J = 4.0 Hz, 1H, Ar), 3.60 (m, 2H, CH_2), 3.0 (m, 2H, CH_2), 2.15 (m, 2H, CH_2); ^{13}C NMR (50 MHz, $CDCl_3$): δ 191.5 (CO), 145.8 (C–CO), 132.2 (CH), 131.4 (CH), 122.9 (C–Br), 44.5 (CH_2), 35.3 (CH_2), 26.9 (CH_2); m/z (EI): 270, 268, 266 (M^+, 4, 13, 10%), 191, 189 (M–$CH_2CH_2CH_2Cl$, 100, 100%); HPLC: Column μ Bondapack C18, 10 μm, 125 Å, (300 × 3.9 mm), purity 99%, rt = 5.85 min, acetonitrile/H_2O (0.05% H_3PO_4 + 0.04% Et_3N) 50/50. Anal. Calcd for $C_8H_8BrClOS$: C, 35.91; H, 3.01; S, 11.98. Found: C, 35.78; H, 2.89; S, 11.90.

4.1.1.3. 2-Bromo-1-(3,4-dibromothiophen-2-yl)ethanone (39).

Bromoacetyl bromide (2.40 g, 0.012 mol), anhydrous $AlCl_3$ (1.57 g, 0.012 mol), 3,4-dibromothiophene (2.5 g, 0.010 mol) and dry CS_2 (50 mL). Purified by column chromatography (hexane:ethyl acetate 8:1), 3.60 g (96%), colorless solid, mp 82–83 °C. ^{1}H NMR (200 MHz, $CDCl_3$): δ 7.71 (s, 1H, Ar), 4.62 (s, 2H, CH_2); ^{13}C NMR (75 MHz, $CDCl_3$): δ 181.5 (CO), 140.2 (C–CO), 131.3 (CH), 119.2, 118.5 (C–Br), 32.8 (CH_2); m/z (EI): 366, 364, 362, 360 (M^+, 4, 10, 4, 10%), 271, 269, 267 (M–CH_2Br, 52, 100, 52%); HPLC: Column μ Bondapack C18, 10 μm, 125 Å, (300 × 3.9 mm), purity 99%, rt = 4.00 min, acetonitrile/H_2O (0.05% H_3PO_4 + 0.04% Et_3N) 50/50. Anal. Calcd for $C_6H_3Br_3OS$: C, 19.86; H, 0.83; S, 8.84. Found: C, 19.79; H, 0.70; S, 8.69.

4.1.1.4. 2-Bromo-1-(4,5-dibromothiophen-2-yl)ethanone (40).

Bromoacetyl bromide (0.95 g, 4.74 mmol), anhydrous $AlCl_3$ (0.63 g, 4.74 mmol), 2,3-dibromothiophene (1.0 g, 4.13 mmol) and dry CS_2 (50 mL). Purified by column chromatography (hexane:ethyl acetate 9:1), 1.39 g (93%), colorless solid, mp: 67–68 °C. ^{1}H NMR (200 MHz, $CDCl_3$): δ 7.59 (s, 1H, Ar), 4.27 (s, 2H, CH_2); ^{13}C NMR (75 MHz, $CDCl_3$): δ 182.9 (CO), 141.0 (C–CO), 135.5 (CH), 123.4, 115.6 (C–Br), 29.4 (CH_2); m/z (EI): 366, 364, 362, 360 (M^+, 4, 10, 4, 10%), 271, 269, 267 (M–CH_2Br, 52, 100, 52%); HPLC: Column μ Bondapack C18, 10 μm, 125 Å, (300 × 3.9 mm), purity 98%, rt = 4.20 min, acetonitrile/H_2O (0.05% H_3PO_4 + 0.04% Et_3N) 50/50. Anal. Calcd for $C_6H_3Br_3OS$: C, 19.86; H, 0.83; S, 8.84. Found: C, 19.69; H, 0.74; S, 8.64.

4.1.1.5. 2-Bromo-1-(5-bromothiophen-2-yl)ethanone (41).

Bromoacetyl bromide (1.91 g, 9.50 mmol), anhydrous $AlCl_3$ (1.26 g, 9.50 mmol), 2-bromothiophene (2.0 g, 8.26 mmol) and dry CS_2 (50 mL). Purified by column chromatography (hexane:ethyl acetate 8:1), 0.64 g (42%), colorless solid, mp 90–91 °C. ^{1}H NMR (200 MHz, $CDCl_3$): δ 7.57 (d, J = 4.02 Hz, 1H, Ar), 7.17 (d, J = 4.02 Hz, 1H, Ar), 4.30 (s, 2H, CH_2); ^{13}C NMR (75 MHz, $CDCl_3$): δ 183.6 (CO), 142.2 (C–CO), 133.8, 131.6 (CH), 124.6 (C–Br), 29.8 (CH_2); m/z (EI): 286, 284, 282 (M^+, 14, 26, 13%), 191, 189 (M–CH_2Br, 99, 100%); HPLC: Column μ Bondapack C18, 10 μm, 125 Å, (300 × 3.9 mm), purity 98%, rt = 4.78 min, acetonitrile/H_2O (0.05% H_3PO_4 + 0.04% Et_3N) 50/50. Anal. Calcd for $C_6H_4Br_2OS$: C, 25.38; H, 1.42; S, 11.29. Found: C, 25.29; H, 1.49; S, 11.40.

4.1.1.6. 2-Bromo-1-(3,5-dibromothiophen-2-yl)ethanone (42).

Bromoacetyl bromide (0.32 g, 1.59 mmol), anhydrous $AlCl_3$ (0.21 g, 1.59 mmol), 2,4-dibromo thiophene (0.35 g, 1.45 mmol) and dry CS_2 (50 mL). Purified by column chromatography (hexane:ethyl acetate 7:1), 0.39 g (72%), colorless solid, mp 75–76 °C. ^{1}H NMR (200 MHz, $CDCl_3$): δ 7.22 (s,1H, Ar), 4.53 (s, 2H, CH_2); ^{13}C NMR (75 MHz, $CDCl_3$): δ 182.8 (CO), 141.4 (C–CO), 136.2 (CH), 123.8, 114.8 (C–Br), 32.9 (CH_2); m/z (EI): 366, 364, 362, 360 (M^+, 7, 20, 7, 20%), 271, 269, 267 (M–CH_2Br, 61, 100, 61%); HPLC: Column μ Bondapack C18, 10 μm, 125 Å, (300 × 3.9 mm), purity 99%, rt = 4.23 min, acetonitrile/H_2O (0.05% H_3PO_4 + 0.04% Et_3N) 50/50. Anal. Calcd for $C_6H_3Br_3OS$: C, 19.86; H, 0.83; S, 8.84. Found: C, 19.81; H, 0.77; S, 8.78.

4.1.1.7. 4-Chloro-1-(2,5-dichlorothiophen-3-yl)butan-1-one (43).

4-Chlorobutyryl chloride (3.24 g, 0.023 mol), anhydrous $AlCl_3$ (3.06 g, 0.023 mol), 2,5-dichlorothiophene (3.06 g, 0.020 mol) and dry CS_2 (50 mL). Purified by column chromatography (hexane:ethyl acetate 4:1), 2.10 g (41%), oil. ^{1}H NMR (200 MHz, $CDCl_3$): δ 7.20 (s, 1H, Ar), 3.70 (m, 2H, CH_2), 3.14 (m, 2H, CH_2), 2.20 (m, 2H, CH_2); ^{13}C NMR (50 MHz, $CDCl_3$): δ 192.0 (CO), 136.6 (C–CO), 132.3 (C–Cl), 130.0 (C–Cl), 126.9 (CH), 44.4 (CH_2), 38.9 (CH_2), 26.4 (CH_2); m/z (EI): 262, 260, 258, 256 (M^+, 1, 4, 10, 9%), 183, 181, 179 (M–$CH_2CH_2CH_2Cl$, 18, 79, 100%); HPLC: Column μ Bondapack C18, 10 μm, 125 Å, (300 × 3.9 mm), purity 98%, rt = 5.46 min, acetonitrile/H_2O (0.05% H_3PO_4 + 0.04% Et_3N) 50/50. Anal. Calcd for $C_8H_7Cl_3OS$: C, 37.31; H, 2.74; S, 12.45. Found: C, 37.40; H, 2.64; S, 12.42.

4.1.2. 2-(2,5-Dichlorothiophen-3-yl)-2-oxoethyl acetate (44)

To a solution of 2-chloro-1-(2,5-dichlorothiophen-3-yl) ethanone (**35**) (0.2 g, 1.31 mmol) in acetic acid (50 mL) was added sodium acetate (0.32 g, 3.94 mmol) and acetic anhydride (0.27 g, 3.94 mmol). The mixture was stirred and refluxed for 5 h. CH_2Cl_2 (100 mL) and H_2O (100 mL) was added to the reaction. The organic layer was washed with H_2O (2 × 100 mL), a saturated solution of $NaHCO_3$ (100 mL) and a saturated solution of NaCl (100 mL). The organic layer was dried over magnesium sulfate and the solvent was evaporated. Compound **44** was purified by column chromatography (hexane:ethyl acetate 7:1), 0.30 g (91%), oil. ^{1}H NMR (200 MHz, $CDCl_3$): δ 7.28 (s, 1H, Ar), 5.22 (s, 2H, CH_2), 2.25 (s, 3H, CH_3); ^{13}C NMR (50 MHz, $CDCl_3$): δ 184.5 (CO), 169.2 (CO), 133.6 (C–CO), 132.0 (C–Cl), 126.7(C–Cl), 125.5 (CH), 66.6 (CH_2), 19.4 (CH_3); m/z (EI): 256, 254, 252, (M^+, 5, 27, 54%), 185, 183 (M–$C_3H_5O_2$, 100, 100%); HPLC: Column Symmetry C18, 5 μm, 100 Å, (150 × 3.9 mm), purity 99%, rt = 8.96 min, acetonitrile/H_2O (0.05% H_3PO_4 + 0.04% Et_3N) 50/50. Anal. Calcd for $C_8H_6Cl_2O_3S$: C, 37.96; H, 2.39. Found: C, 37.89; H, 2.42.

4.1.3. Chemical reactivity of HMKs

Hundred microliters of an acetonitrile solution of HMK **29** (50 mM) and 100 μL of an acetonitrile solution of 2-mercap-

toethanol (50 mM) were added to a mixture of methanol/water (1/1, 0.8 mL) and stirred for 30 min or 18 h. The reaction progress was followed by HPLC–MS injecting aliquots after 30 min or 18 h. HMK **29** (MW = 195) showed a retention time of 4.80 min, while the S-alkylated derivative (MW = 236) presented a retention time of 4.06 min. Additional experiment was carried out when the 2-mercaptoethanol concentration was increased 10 times. In this case 100 μL of an acetonitrile solution of 2-mercaptoethanol (500 mM) was added. The same procedure described above was followed when triethylamine was used. In this case, 100 μL of an acetonitrile solution of triethylamine (50 mM) was added to a methanol/water (1/1, 0.7 mL) solution.

4.2. Biological studies

4.2.1. Inhibition of GSK-3

GSK-3β enzyme (Sigma) was incubated with 15 μM of ATP, 0.2 μCi of [γ-^{32}P]ATP, GS-1 substrate, and different concentration of test compound. GSK-3β activity was assayed in 50 mM tris, pH 7.5, 10 mM $MgCl_2$, 1 mM EGTA and 1 mM EDTA buffer at 37 °C, in the presence of 15 mM GS-1 (substrate), 15 μM of ATP, 0.2 μCi of [γ-^{32}P] ATP in a final volume of 12 μL. After 20 min of incubation at 37 °C, 4 μL aliquots of the supernatant were spotted onto 2x2 pieces of Whatman P81 phosphocellulose paper, and the filter was washed four times (at least 10 min each time) in 1% phosphoric acid. The dried filters were transferred into scintillation vials, and the radioactivity was measured in a liquid scintillation counter. Blank values were subtracted, and the GSK-3β activity was expressed in percentage of maximal activity. The IC_{50} is defined as the concentration of each compound that reduces enzyme activity by 50% with respect to that without inhibitor present.

4.2.2. Reversibility inhibition studies of GSK-3

Immobilized recombinant histidine-tagged GSK-3β on a nickel agarose gel (Sigma) was incubated with 15 μM of ATP, 0.2 μCi of [γ-^{32}P]ATP, GS-1 substrate, and different concentration of test compounds. GSK-3β activity was assayed in 50 mM tris, pH 7.5, 10 mM $MgCl_2$, 1 mM EGTA and 1 mM EDTA buffer at 37 °C, in a final volume of 20 μL. After 20 min of incubation at 37 °C, the reaction mixture was centrifuged at 12,000 rpm. for 5 min at 4 °C. The supernatant was collected to evaluate the radioactivity incorporated in the GS-1 peptide. Thus, a 4 μL aliquot of the supernatant were spotted onto 2 × 2 pieces of Whatman P81 phosphocellulose paper, and the filter was washed four times (at least 10 min each time) in 1% phosphoric acid. The dried filters were transferred into scintillation vials, and the radioactivity was measured in a liquid scintillation counter. Blank values were subtracted, and the GSK-3β activity was expressed in percentage of maximal activity.

On the other hand, the pellet with the immobilized GSK-3 on the nickel agarose gel was washed three times (at least 10 min each time) with abundant volume of 50 mM tris, pH 7.5, 10 mM $MgCl_2$ buffer, to eliminate the inhibitor unbounded to the enzyme. After the last washing, the pellet enzymatic activity was determined in 50 mM tris, pH 7.5, 10 mM $MgCl_2$, 1 mM EGTA and 1 mM EDTA buffer containing 15 μM of ATP, 0.2 μCi of [γ-^{32}P]ATP, and 15 mM GS-1 substrate. After 15 min incubation the radioactivity incorporated in the GS-1 peptide was determined following the method above described. The GSK-3β activity in the presence of the compound is expressed as a percentage of the GSK-3β activity of the control without the compound but with the same work-up.

A second study was performed to determine the irreversibility of HMK inhibition. Thus, GSK-3β enzyme (Sigma) was incubated in a buffer containing 20 mM Tris, pH 7.4, for 30 min, before determine its activity, with HMK **32**, at a final concentration of 10 μM. This concentration was previously determined to produce the maximal inhibition. After that, the activity of GSK-3β, treated with HMK **32** or without any inhibitor (control), diluted 20 times in kinase buffer, and maintained for 30 min to equilibrate the different components, was determined. In parallel, the control reaction (GSK-3 without inhibitor) was incubated at a final concentration of HMK **32** similar to those obtained after dilution (0.5 μM); or low lithium chloride concentration. The final kinase activity was assayed over Myelin basic protein (MBP), as described below.

4.2.3. Derivatization of sulfhydryl groups of GSK-3

The sulfhydryl groups were derivatized by reaction with 15 mM iodoacetamide in a buffer containing 50 mM tris, pH 7.4, 1 mM EGTA. GSK-3β enzyme (Sigma) was incubated in this buffer, for 20 or 30 min and then the kinase activity was assayed. GSK-3β enzyme (Sigma) derivatized with iodoacetamide or without any modification was assayed for its kinase activity.

GSK-3β activity was determined in 50 mM tris, pH 7.5, 10 mM MgCl2, 1 mM EGTA buffer (kinase buffer) at 37 °C, in the presence of 4 μg of myelin basic protein (MBP) as substrate, 15 μM of ATP, 0.2 μCi of [γ-^{32}P] ATP in a final volume of 25 μl. As an internal control, the inhibitory capacity of HMK **32** or lithium chloride was used as reference.

4.2.4. Neurotransmitter receptors binding assays

The neurotransmitter binding assays are described in each paragraph:

- α-2 (Non-selective) adrenergic receptor:[39] From rat cerebral cortex, yohimbine was used as reference compound and [^{3}H] RX 821002 as a ligand (0.5 nM).
- D2 (*h*) dopamine receptor:[40] Human recombinant (CHO cells), (+)-buctaclamol was used as reference compound and [^{3}H] spiperone as a ligand (0.3 nM).
- D3 (h) dopamine receptor:[41] Human recombinant (CHO cells), (+)-buctaclamol was used as reference compound and [^{3}H] spiperone as a ligand (0.3 nM).
- AMPA glutaminergic receptor:[42] From rat cerebral cortex, L-glutamate was used as reference compound and [^{3}H] AMPA as a ligand (8 nM).
- NMDA glutaminergic receptor:[43] From rat cerebral cortex, CGS 19755 was used as reference compound and [^{3}H] CGP 39653 as a ligand (5 nM).
- M (non-selective) muscarinic receptor:[44] From rat cerebral cortex, atropine was used as reference compound and [^{3}H] QNB as a ligand (0.05 nM).
- N (neuronal) (α-BGTX-insensitive) nicotinic receptor:[45] From rat cerebral cortex, nicotine was used as reference compound and [^{3}H] cytisine as a ligand (1.5 nM).
- N (neuronal) (α-BGTX-sensitive) nicotinic receptor:[46] From rat cerebral cortex, α-bungarotoxin was used as reference compound and [^{125}I] α-bungarotoxin as a ligand (1 nM).
- 5-HT (non-selective) serotoninergic receptor:[47] From rat cerebral cortex, serotonine was used as reference compound and [^{3}H] serotonine as a ligand (2 nM).

4.2.5. Inhibition of protein kinases

The experimental procedures for the inhibition of different protein kinases are described in each paragraph:

- Abl kinase:[48] Mouse recombinant (*E. coli*), staurosporine was used as reference compound and poly GT (0.4 μg.mL^{-1}) as a substrate. Fluorescence polarization was used as the method of detection for the reaction product (phosphopolyGT).

- CAM kinase II:[49] From rat brain, staurosporine was used as reference compound and [γ^{33}-P] ATP + autocamtide-2 (5 μM) as a substrate. Liquid scintillation was used as method of detection for the reaction product ([γ^{33}-P] autocamtide-2).
- EGFR kinase:[50] From A-431 cells, PD 153035 was used as reference compound and [γ^{33}-P] ATP + poly GAT (0.48 mg mL^{-1}) as a substrate. Liquid scintillation was used as method of detection for the reaction product ([γ^{33}-P] poly GAT).
- IR-K (*h*):[51] Human recombinant, staurosporine was used as reference compound and [γ^{33}-P] ATP + poly GT (0.03 mg.mL^{-1}) as a substrate. Liquid scintillation was used as method of detection for the reaction product ([γ^{33}-P] poly GT).
- MAP kinase (ERK 42):[52] Rat recombinant (*E. coli*), staurosporine was used as reference compound and [γ^{33}-P] ATP + MBP (0.5 mg mL^{-1}) as a substrate. Liquid scintillation was used as method of detection for the reaction product ([γ^{33}-P] MBP).
- MEK1 kinase:[53] Rabbit recombinant (E.coli), staurosporine was used as reference compound and ATP + unactivated MAP kinase (0.01 mg mL^{-1}) as a substrate. Liquid scintillation was used as method of detection for the reaction product ([γ^{33}-P] MBP).
- Protein kinase $p56^{lck}$:[54] From bovine thymus, staurosporine was used as reference compound and [γ^{33}-P] ATP + poliGT (0.5 mg mL^{-1}) as a substrate. Liquid scintillation was used as method of detection for the reaction product ([γ^{33}-P] polyGT).

4.2.6. Neuronal cell cultures and treatments

Neuro2A mouse neuroblastoma cells were routinely grown in Dulbecco's modified Eagle's medium (DMEM) with 10% heat-inactivated fetal calf serum containing glutamine (2 mM) and antibiotics (Pen./Strept.).

To obtain a neuronal-like phenotype, cells were maintained for 24–48 h in serum-free neurobasal medium supplemented with B-27 (NB-B27). Alternatively N2A have specific properties and neuronal-like phenotype may be induced by addition of lithium chloride 10 mM, in the growing media (DEMEN-10%FCS). The effect was analyzed 24 h after addition. Similarly, some HMKs were assayed for the potential effect of producing neurite extension as lithium chloride did, and the compounds were added as indicated for 16 h.

Granule cerebellar neurons (GCNs) were obtained as described previously.[55] Briefly, cerebellar granule neurons were isolated from postnatal day 6 (P6) mice as described. The cells were plated onto poly-L-lysine coated dishes and grown for 48 h in serum-free neurobasal medium supplemented with B-27 and 12.5 mM KCl.

Lithium chloride (Sigma) was used in this study as the GSK-3 kinase inhibitor.[56] As lithium also inhibits inositol monophosphatase, all of our experiments with lithium were performed in the presence of an excess of myo-inositol to avoid the effects provoked by inositol depletion.

The inhibition of GSK-3 was inferred from tau phosphorylation and the effects were compared with parallel cultures that were exposed to selected HMKs, at different concentration (ranging from 0.5 to 25 μM).

4.2.7. Antibodies and Western blot analysis

The antibodies used in this study were: anti-β-actin mAb (Sigma); PHF-1, which is an antiphospho $Ser^{396/404}$ Tau mAb (kindly supplied by Dr. P. Davies, Albert Einstein Coll, Bronx, NY, USA); and Tau monoclonal antibody Tau-1, from Chemicon, recognizes Residues Ser 195,198,199,202 non-phosphorylated.

Cell extracts were prepared from cells washed with 1× PBS and then resuspended in a buffer containing: 20 mM HEPES, pH 7.4; 100 mM NaCl; 100 mM NaF; 1 mM sodium *ortho*-vanadate; 5 mM EDTA; Okadaic Acid 1 μM; 1% Triton X-100; and a protease inhibitor cocktail (Complete, Roche). The soluble fraction was obtained by centrifugation at 14,000*g* for 10 min at 4 °C, and the proteins (10–50 μg) were separated by SDS–PAGE before being transferred to a nitrocellulose filter. The filters were blocked with 5% non-fat milk in PBS, 0.1% Tween-20 (PBS-T) and then incubated with primary antibodies overnight at 4 °C. Subsequently, the filters were rinsed three times in PBST buffer before being exposed to the corresponding peroxidase-conjugated secondary antibody (diluted 1:5000, Promega) for 1 h at room temperature. Immunoreactivity was visualized using an enhanced chemiluminescence detection system (Perkin–Elmer Life Sci.). Each experiment was normalized with respect to the amount of actin present in each cell extract. The data are expressed as the mean of three independent experiments and the data from control cells were considered 100 relative unit (r.u.).

4.3. Molecular modeling. CMIP calculations

Preferential binding sites of HMKs on GSK-3 protein surface were obtained using the docking module of the program CMIP. The protein (PDB entry 1I09) was mapped onto a 3D grid of the appropriate size with a 0.5 Å regular spacing (ca. 4,000,000 grid positions). Binding was assayed by exhaustive search of 8000 orientations (using non-redundant Euler angles) for every grid position. When necessary, flexible molecules were assayed as a family of standard rotamers. Docked positions were scored using interaction energies between the ligand and the protein, which were evaluated by adding electrostatic and van der Waals contributions. The solvent-screened electrostatic interaction was determined by using the Mehler-Solmajer sigmoidal distance-dependent dielectric model,[57] and the van der Waals component was evaluated by using a Lennard–Jones expression. Parameters for protein atoms were obtained from the amber98 force field.[58] For the ligand molecules, RESP atomic charges determined at the HF/6-31G(d) level were used in conjunction with van der Waals parameters taken for related atoms in the amber98 force field. Finally, refinement of the binding mode was carried out by means of docking computations with the program rDock, which is an extension of the program RIBODOCK[59] using an empirical scoring function calibrated based on protein–ligand complexes.[60] To this end, 100 docking computations were run, and the output docking modes were analyzed by visual inspection in conjunction with the docking scores.

Acknowledgement

We acknowledge partial financial support from NeuroPharma (currently named NOSCIRA).

Supplementary data

Supplementary data associated with this article can be found, in the online version, at doi:10.1016/j.bmc.2009.08.042.

References and notes

1. Cohen, P. *Nat. Rev. Drug Disc.* **2002**, *1*, 309.
2. Sawa, M. *Mini-Rev. Med. Chem.* **2008**, *8*, 1291.
3. Hochhaus, A. *J. Natl. Compr. Canc. Netw.* **2008**, *6*(Suppl 2), S1.
4. Danovi, S. A.; Wong, H. H.; Lemoine, N. R. *Br. Med. Bull.* **2008**, *87*, 97.
5. Noble, M. E.; Endicott, J. A.; Johnson, L. N. *Science* **2004**, *303*, 1800.
6. Schmidt, R.; Neff, F.; Lampl, C.; Benke, T.; Anditsch, M.; Bancher, C.; Dal-Bianco, P.; Reisecker, F.; Marksteiner, J.; Rainer, M.; Kapeller, P.; Dodel, R. *Neuropsychiatr.* **2008**, *22*, 153.
7. Hooper, C.; Killick, R.; Lovestone, S. *J. Neurochem.* **2008**, *104*, 1433.
8. *In Glycogen Synthase Kinase 3 and its Inhibitors*; Martinez, A., Castro, A., Medina, M., Eds.; John Wiley & Sons: New Jersey, 2006.
9. Huang, H. C.; Klein, P. S. *Curr. Drug Targets* **2006**, *7*, 1389.
10. Cohen, P.; Goedert, M. *Nat. Rev. Drug Disc.* **2004**, *3*, 479.
11. Martinez, A. *Med. Res. Rev.* **2008**, *28*, 773.
12. Martinez, A.; Perez, D. I. *J. Alzheimers Dis.* **2008**, *15*, 181.

13. A. Martinez, M. Alonso, A. Castro, I. Dorronsoro, in: A.E. Martinez (Ed.), Medicinal Chemistry of Alzheimer's disease, Transworld Research Network: Kerala, 2008; p 225.
14. Castro, A.; Conde, S.; Rodriguez-Franco, M. I.; Martinez, A. *Mini-Rev. Med. Chem.* **2002**, *2*, 37.
15. Castro, A.; Martinez, A. *Mini-Rev. Med. Chem.* **2001**, *1*, 267.
16. Martinez, A.; Alonso, M.; Castro, A.; Perez, C.; Moreno, F. J. *J. Med. Chem.* **2002**, *45*, 1292.
17. Conde, S.; Perez, D. I.; Martinez, A.; Perez, C.; Moreno, F. J. *J. Med. Chem.* **2003**, *46*, 4631.
18. Woodgett, J. R. *Anal. Biochem.* **1989**, *180*, 237.
19. Martinez, A.; Alonso, M.; Castro, A.; Dorronsoro, I.; Gelpi, J. L.; Luque, F. J.; Perez, C.; Moreno, F. J. *J. Med. Chem.* **2005**, *48*, 7103.
20. Rosenfeld, R.; Vajda, S.; DeLisi, C. *Annu. Rev. Biophys. Biomol. Struct.* **1995**, *24*, 677.
21. Ahn, N. G.; Resing, K. A. *Science* **2005**, *308*, 1266.
22. Gattis, J. L.; Ruben, E.; Fenley, M. O.; Ellington, W. R.; Chapman, M. S. *Biochemistry* **2004**, *43*, 8680.
23. Anselmo, A. N.; Cobb, M. H. *Biochem. J.* **2004**, *381*, e1.
24. Vulpetti, A.; Crivori, P.; Cameron, A.; Bertrand, J.; Brasca, M. G.; D'Alessio, R.; Pevarello, P. *J. Chem. Inf. Model.* **2005**, *45*, 1282.
25. Rauber, P.; Angliker, H.; Walker, B.; Shaw, E. *Biochem. J.* **1986**, *239*, 633.
26. Drenth, J.; Kalk, K. H.; Swen, H. M. *Biochemistry* **1976**, *15*, 3731.
27. Rahman, M. A.; Senga, T.; Oo, M. L.; Hasegawa, H.; Biswas, M. H.; Mon, N. N.; Huang, P.; Ito, S.; Yamamoto, T.; Hamaguchi, M. *Oncol. Rep.* **2008**, *19*, 975.
28. Mazanetz, M. P.; Fischer, P. M. *Nat. Rev. Drug Disc.* **2007**, *6*, 464.
29. Dajani, R.; Fraser, E.; Roe, S. M.; Young, N.; Good, V.; Dale, T. C.; Pearl, L. H. *Cell* **2001**, *105*, 721.
30. Kockeritz, L.; Doble, B.; Patel, S.; Woodgett, J. R. *Curr. Drug Targets* **2006**, *7*, 1377.
31. Orme, M. H.; Giannini, A. L.; Vivanco, M. D.; Kypta, R. M. *Mol. Cell Neurosci.* **2003**, *24*, 673.
32. Di, L.; Kerns, E. H. *Curr. Opin. Chem. Biol.* **2003**, *7*, 402.
33. Veber, D. F.; Johnson, S. R.; Cheng, H.-Y.; Smith, B. R.; Ward, K. W.; Kopple, K. D. *J. Med. Chem.* **2002**, *45*, 2615.
34. Dorronsoro, I.; Chana, A.; Abasolo, I.; Castro, A.; Gil, C.; Stud, M.; Martinez, A. *QSAR Comb. Sci.* **2004**, *23*, 89.
35. Powers, J. C.; Asgian, J. L.; Ekici, O. D.; James, K. E. *Chem. Rev.* **2002**, *102*, 4639.
36. Yasuda, S.; Liang, M.-H.; Marinova, Z.; Yahyavi, A.; Chuang, D.-M. *Mol. Psychiatry* **2009**, *14*, 51.
37. Lochhead, P. A.; Kinstrie, R.; Sibbet, G.; Rawjee, T.; Morrice, N.; Cleghon, V. *Mol. Cell* **2006**, *24*, 627.
38. Li, Z.; Tan, F.; Thiele, C. J. *Mol. Cancer Ther.* **2007**, *6*, 3113.
39. Uhlen, S.; Wikberg, J. E. *Pharmacol. Toxicol.* **1991**, *69*, 341.
40. Grandy, D. K.; Marchionni, M. A.; Makam, H.; Stofko, R. E.; Alfano, M.; Frothingham, L.; Fischer, J. B.; Burke-Howie, K. J.; Bunzow, J. R.; Server, A. C., et al *Proc. Natl. Acad. Sci. U.S.A.* **1989**, *86*, 9762.
41. MacKenzie, R. G.; VanLeeuwen, D.; Pugsley, T. A.; Shih, Y. H.; Demattos, S.; Tang, L.; Todd, R. D.; O'Malley, K. L. *Eur. J. Pharmacol.* **1994**, *266*, 79.
42. Murphy, D. E.; Snowhill, E. W.; Williams, M. *Neurochem. Res.* **1987**, *12*, 775.
43. Sills, M. A.; Fagg, G.; Pozza, M.; Angst, C.; Brundish, D. E.; Hurt, S. D.; Wilusz, E. J.; Williams, M. *Eur. J. Pharmacol.* **1991**, *192*, 19.
44. Richards, M. H. *Br. J. Pharmacol.* **1990**, *99*, 753.
45. Pabreza, L. A.; Dhawan, S.; Kellar, K. J. *Mol. Pharmacol.* **1991**, *39*, 9.
46. Sharples, C. G.; Kaiser, S.; Soliakov, L.; Marks, M. J.; Collins, A. C.; Washburn, M.; Wright, E.; Spencer, J. A.; Gallagher, T.; Whiteaker, P.; Wonnacott, S. *J. Neurosci.* **2000**, *20*, 2783.
47. Peroutka, S. J.; Snyder, S. H. *Mol. Pharmacol.* **1979**, *16*, 687.
48. Parker, G. J.; Law, T. L.; Lenoch, F. J.; Bolger, R. E. *J. Biomol. Screen.* **2000**, *5*, 77.
49. Lengyel, I.; Nairn, A.; McCluskey, A.; Toth, G.; Penke, B.; Rostas, J. *J. Neurochem.* **2001**, *76*, 1066.
50. Carpenter, G.; King, L., Jr.; Cohen, S. *J. Biol. Chem.* **1979**, *254*, 4884.
51. Al-Hasani, H.; Passlack, W.; Klein, H. W. *FEBS Lett.* **1994**, *349*, 17.
52. Robbins, D. J.; Zhen, E.; Owaki, H.; Vanderbilt, C. A.; Ebert, D.; Geppert, T. D.; Cobb, M. H. *J. Biol. Chem.* **1993**, *268*, 5097.
53. Williams, D. H.; Wilkinson, S. E.; Purton, T.; Lamont, A.; Flotow, H.; Murray, E. J. *Biochemistry* **1998**, *37*, 9579.
54. Cheng, H. C.; Nishio, H.; Hatase, O.; Ralph, S.; Wang, J. H. *J. Biol. Chem.* **1992**, *267*, 9248.
55. Sayas, C. L.; Avila, J.; Wandosell, F. *J. Neurosci.* **2002**, *22*, 6863.
56. Klein, P. S.; Melton, D. A. *Proc. Natl. Acad. Sci. U.S.A.* **1996**, *93*, 8455.
57. Mehler, E. L.; Solmajer, T. *Protein Eng.* **1991**, *4*, 903.
58. Cornell, W. D.; Cieplak, P.; Bayly, C. I.; Gould, I. R.; Merz, K. M.; Ferguson, D. M.; Spellmeyer, D. C.; Fox, T.; Caldwell, J. W.; Kollman, P. A. *J. Am. Chem. Soc.* **1995**, *117*, 5179.
59. Morley, S. D.; Afshar, M. *J. Comput. Aided Mol. Des.* **2004**, *18*, 189.
60. Barril, X.; Hubbard, R. E.; Morley, S. D. *Mini-Rev. Med. Chem.* **2004**, *4*, 779.